A qualitative solution with quantitative potential for the mouse hippocampal cortex flatmap problem

Larry W. Swanson[a,1,2] and Joel D. Hahn[a,1]

[a]Department of Biological Sciences, University of Southern California, Los Angeles, CA 90089

Contributed by Larry W. Swanson, December 12, 2019 (sent for review October 30, 2019; reviewed by Troy Margrie and Thanos Siapas)

The hippocampal formation (HPF) is a focus of intense experimental investigation, particularly because of its roles in conscious memory consolidation, spatial navigation, emotion, and motivated behaviors. However, the HPF has a complex three-dimensional geometry resulting from extreme curvature of its layers, and this presents a challenge for investigators seeking to decipher hippocampal structure and function at cellular and molecular scales (neuronal circuitry, gene expression, and other properties). Previously, this problem was solved qualitatively for the rat by constructing a physical surface model of the HPF based on histological sections, and then deriving from the model a flatmap. Its usefulness is exemplified by previous studies that used it to display topological relationships between different components of intrahippocampal circuitry derived from experimental pathway-tracing experiments. Here the rat HPF flatmap was used as a starting point to construct an analogous flatmap for the mouse, where the great majority of experimental hippocampal research is currently performed. A detailed account of underlying knowledge and principles is provided, including for hippocampal terminology, and development from an embryonic nonfolded sheet into differentiated multiple adjacent cortical areas, giving rise to the adult shape. To demonstrate its utility, the mouse flatmap was used to display the results of pathway-tracing experiments showing the dentate gyrus mossy fiber projection, and its relationship to the intrahippocampal Purkinje cell protein 4 gene-expression pattern. Finally, requirements for constructing a computer graphics quantitative intrahippocampal flatmap, with accompanying intrahippocampal coordinate system, are presented; they should be applicable to all mammals, including human.

dentate gyrus | hippocampus | subiculum | presubiculum | entorhinal area

The hippocampal formation (HPF) is one of the most intensely studied nervous system parts because of the important role it appears to play in various cerebral cortical functions, including conscious memory consolidation (1), spatial navigation (2), and the expression of emotion and motivated behaviors (3, 4). Unfortunately (for neuroscientists), the HPF has by far the most complex spatial arrangement of any major brain part; in all mammals it displays extreme fissuration with corresponding gyration, an overall "C"- or banana-shaped profile when viewed laterally, and an oblique orientation in the right and left hemispheres when viewed from above. These HPF structural features make its basic geometric shapes and their spatial relationships very difficult to comprehend, visualize, and interpret in standard series of transverse (frontal or coronal), sagittal, or horizontal sections through the HPF. This in turn makes it very difficult to elucidate HPF organizing principles (the basic plan), including for its intrinsic and extrinsic circuitry, and related functional subsystems, neuron types, gene-expression patterns, or other cellular and molecular properties.

One solution to the problem of understanding hippocampal structure–function spatial relationships is to create a flatmap from the folded sheet of all cerebral cortical areas forming the HPF, similar in principle to creating a two-dimensional (2D) wall map of the Earth's surface. This type of flatmap was created previously for rat (5–8), and it was instrumental for displaying differential patterns of intrinsic and extrinsic neuronal circuit organization with respect to the HPF longitudinal and transverse axes (see refs. 3, 5, 7, 9, and 10).

The majority of hippocampal research is now being done in mice, driven in part by the power of current genomic and viral pathway-tracing methods engineered for use in these animals. Because a mouse hippocampus flatmap does not exist and may prove useful, and because a quantitative solution to the hippocampal flatmap problem remains unsolved, we describe here our step-by-step qualitative method for generating the rat hippocampus flatmap, and for using it to generate a comparable mouse hippocampal flatmap. This approach is based on the established principle (11) that exploratory, qualitative data analysis is foundational for subsequent quantitative analysis. We also compare mouse and rat HPF spatial properties, and consider attributes required for a quantitative and algorithmic (programable) solution for the mammalian hippocampal flatmap problem.

Introduction to Terminology

The human hippocampus has been known at least since 1587 when Aranzi (12) described a long, curved bulge that is shaped like a seahorse (*hippokampos* in Greek), extending the length of the lateral ventricle inferior horn (Fig. 1). Later in this period of gross anatomical research, Vicq d'Azyr (13) clearly distinguished the dentate gyrus from Ammon's horn (and both parts from the adjacent parahippocampal gyrus) in sections through the temporal

Significance

The hippocampal formation (HPF) plays an important role in many cerebral cortical functions, including memory consolidation, spatial navigation, and motivation and emotion. However, the highly convoluted hippocampal layers make visualization of basic spatial relationships unusually difficult. A mouse HPF flatmap was derived qualitatively from a physical model in rat, and to demonstrate its utility this flatmap was used to compare the results of experiments showing the intrahippocampal projections of dentate gyrus mossy fibers with Pcp4 gene expression. A spatial comparison of the rat and mouse HPF is included, and requirements are presented for producing a quantitative computer graphics flatmap that could be used to create a human hippocampal flatmap with accompanying coordinate system that transfers onto the intact brain.

Author contributions: L.W.S. designed research; L.W.S. and J.D.H. performed research; L.W.S. and J.D.H. analyzed data and created all figures; and L.W.S. wrote the paper with editorial input from J.D.H.

Reviewers: T.M., Sainsbury Wellcome Centre for Neural Circuits & Behavior, University College London; and T.S., California Institute of Technology.

The authors declare no competing interest.

[1]L.W.S. and J.D.H. contributed equally to this work.

[2]To whom correspondence may be addressed. Email: larryswanson10@gmail.com.

This article contains supporting information online at https://www.pnas.org/lookup/suppl/doi:10.1073/pnas.1918907117/-/DCSupplemental.

First published January 27, 2020.

lobe. Eventually, stunning hippocampal cellular architecture was revealed by Golgi (14), and then systematically and critically analyzed by Cajal (15) and his student Lorente de Nó (16, 17).

Beginning with Aranzi (12), an elaborate terminology has evolved to describe the structural organization of the HPF, and the massive white matter fiber system, the fornix, connecting it with subcortical structures (18, 19). Unfortunately, the vagaries of this terminology are no less complex and confusing than those of HPF structural organization. In the following analysis, a modern, internally consistent, and straightforward hierarchically organized nomenclature is used to describe HPF structural organization in mammals, including rats, mice, and humans (Fig. 2). By way of introduction, the mammalian HPF has two great divisions, the hippocampal region and retrohippocampal region. The hippocampal region's main parts are the dentate gyrus and Ammon's horn, whereas the retrohippocampal region's main parts are subicular (subiculum, pre- and postsubiculum, and parasubiculum) and entorhinal area. As we shall see, this series of adjacent cortical areas is united structurally and functionally by the intrahippocampal circuit and its well-known component, the trisynaptic circuit.

Development from a Simple Nonfolded Sheet. A brief consideration of cerebral cortical embryogenesis is helpful because at early stages the presumptive HPF constitutes the medial edge of the yet-to-fold cortical plate, which is generated dorsally in the neural tube's endbrain (telencephalic) vesicle. Very early, before neurogenesis begins, the endbrain vesicle is in appearance simply a thin, contact lens-shaped sheet, making spatial relationships and flatmap comparisons easy to comprehend. These and other basic topological arrangements are shown in Fig. 3, a fate map of the rostral end of the 4-wk human neural tube, although the same relationships presumably apply to mammals generally at this stage of development.

Clearly, the presumptive HPF lies along the endbrain vesicle's medial edge (Fig. 3), including the endbrain ependymal roof plate caudally and ventrally (where the lateral ventricular

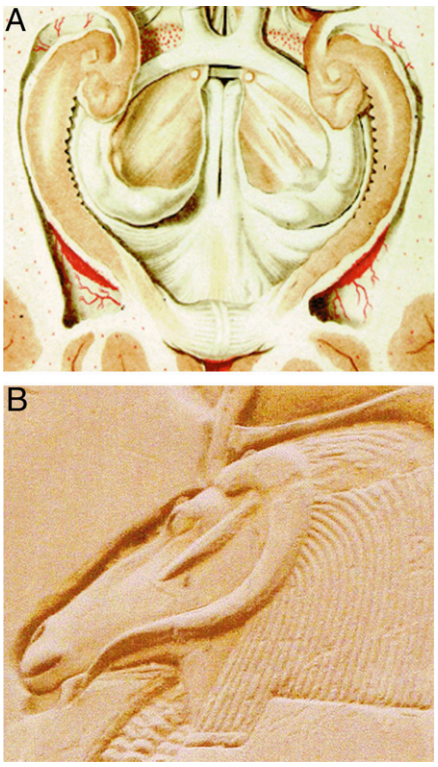

Fig. 1. Origins of hippocampal nomenclature. (*A*) Dissection of right and left human hippocampus, with its fanciful resemblance to a seahorse (from ref. 13). Each hippocampus lies medial to the lateral ventricle inferior horn (with its red choroid plexus); the "head" of each hippocampus is formed by the uncus (Latin for "hook") and the serrated medial edge of each hippocampus "body" is aptly named the dentate ("toothed") gyrus. The optic chiasm is in the rostral (anterior) midline (top of the figure), and the corpus callosum splenium is in the caudal (posterior) midline (bottom of the figure). (*B*) Ammon's horn (*cornu Ammonis* in Latin) was named for the ancient Egyptian deity Ammon, who was depicted as a man with the head of ram. This depiction of Ammon's head in relief showing his left horn is from the ancient Egyptian temple complex of Karnak. Image courtesy of Henri Duvernoy (Université de Franche-Comté, Besançon, France).

Hippocampal formation (HPF)
- *Hippocampal region (HIP)*
  - Indusium griseum (IG)
  - Fasciola cinerea (FC)
  - Dentate gyrus (DG)
    - molecular layer (DGmo)
    - granule cell layer (DGgs
    - polymorph layer (DGpo)
  - Ammon's horn (CA, for cornu Ammonis)
    - Field CA3 (CA3)
      - stratum lacunosum-moleculare (CA3slm)
      - stratum radiatum (CA3sr)
      - stratum lucidum (CA3slu)
      - pyramidal layer (CA3sp)
      - stratum oriens (CA3so)
    - Field CA2 (CA2)
      - stratum lacunosum-moleculare (CA2slm)
      - stratum radiatum (CA2sr)
      - pyramidal layer (CA2sp)
      - stratum oriens (CA2so)
    - Field CA1 (CA1)
      - Field CA1 ventral part (CA1v)
        - stratum lacunosum-moleculare (CA1v-slm)
        - stratum radiatum (CA1v-sr)
        - deep pyramidal layer (CA1v-spd)
        - superficial pyramidal layer (CA1v-sps)
        - stratum oriens (CA3v-so)
      - Field CA1 dorsal part (CA1d)
        - stratum lacunosum-moleculare (CA1d-slm)
        - stratum radiatum (CA1d-sr)
        - deep pyramidal layer (CA1d-sp)
        - superficial pyramidal layer (CA1d-sps)
        - stratum oriens (CA1d-so)
- *Retrohippocampal region (RHP)*
  - Subiculum (SUB)
    - Subiculum ventral part (SUBv)
      - molecular layer (SUBv-m)
      - stratum radiatum (SUBv-sr)
      - pyramidal layer (SUBv-sp)
    - Subiculum dorsal part (SUBd)
      - molecular layer (SUBd-m)
      - stratum radiatum (SUBd-sr)
      - pyramidal layer (SUBd-sp)
  - Presubiculum (PRE)
    - layers 1-6 (PRE1-6)
  - Postsubiculum (POST)
    - layers 1-6 (POST1-6)
  - Parasubiculum (PAR)
    - layers 1-6 (POST1-6)
  - Entorhinal area (ENT)
    - Entorhinal area medial part (ENTm)
      - layers 1-6 (ENTm1-6)
    - Entorhinal area lateral part (ENTl)
      - layers 1-6 (ENTl1-6)

Fig. 2. A standard HPF nomenclature scheme. The basic hierarchical organization was developed for mammals (28), and has been applied to rat (6), mouse (34), and human (19). This version is adapted from the current (fourth) edition of the rat brain atlas, *Brain Maps* (8), where gray matter regions occupying the lowest basic hierarchical level (red text) may be thought of as roughly analogous to the species level in biological taxonomy, providing a brain-wide reference nomenclature that is useful for multiple types of analyses including connectomics.

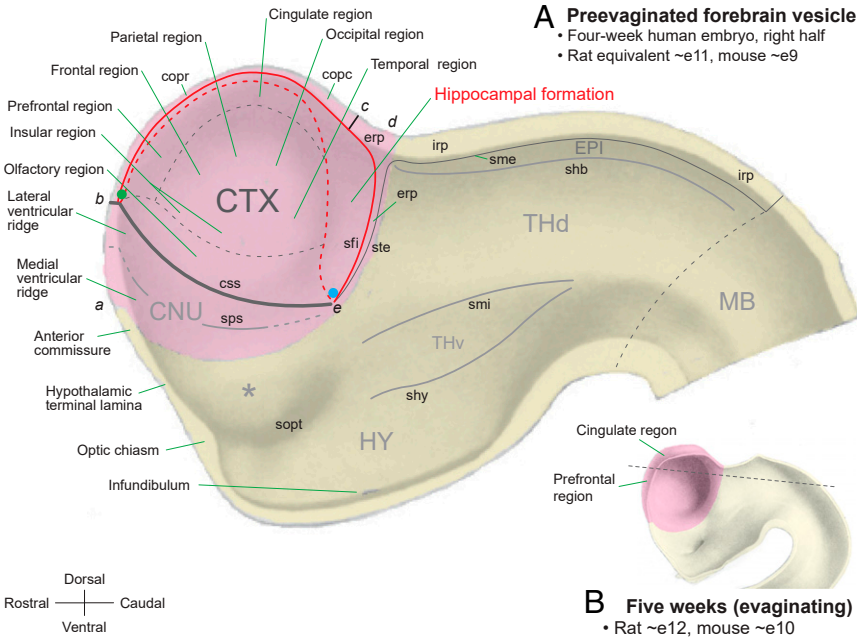

Fig. 3. A fate map model of the human neural tube's forebrain vesicle to show presumptive topological relationships between HPF and other endbrain (pink) and interbrain (yellow) parts at their earliest stages of development. (*A*) Depiction of a rostral portion of the neural tube's right half, transected at the midbrain vesicle and sliced lengthwise along the median plane, revealing the inner surface and midsagittal part of the neural tube's wall. The portion shown illustrates the forebrain vesicle at ~4 wk of gestation, before extensive cortical evagination, and then fissuration, begin. The endbrain vesicle's outward (lateral, into the page) bulge at this stage is contact lens-shaped and its entire medial edge (*a, b, c, d, e, a*) forms a ring (limbus) that soon begins to evaginate; see (*B*) for the beginning of this extensive process. The dashed line in (*B*) indicates the approximate viewing angle of Fig. 4*A*. At this embryonic stage the distinction between endbrain and interbrain is indicated by an external groove (hemispheric sulcus, not shown), and a corresponding internal bulge (torus hemisphericus, not labeled); at later stages (see Fig. 4*A*), the endbrain is associated with lateral ventricle and interbrain is associated with third ventricle. As development progresses from the fourth week of gestation, and neurogenesis begins, the endbrain vesicle becomes divided by the corticostriatal sulcus (css) into the cerebral cortex (CTX) dorsally and cerebral nuclei (CNU) ventrally. A series of sulci (see labels) also begins to divide the interbrain into its major subdivisions: The hypothalamus (HY), ventral thalamus (THv), dorsal thalamus (THd), and epithalamus (EPI). This figure relies heavily on the histological analyses in refs. 26 and 38, and on the terminology defined in ref. 19; the figure is adapted with permission from ref. 48. Abbreviations: *a-e*, medial edge of endbrain vesicle adjacent to interbrain vesicle (yellow); copc, commissural plate of endbrain roof plate (between *b* and *c*), caudal part for hippocampal commissures, dorsal commissure rostrally, ventral commissure caudally; copr, commissural plate of endbrain roof plate (between *b* and *c*), rostral part for corpus callosum; erp, endbrain (telencephalic) ependymal roof plate (between *c–e*); irp, interbrain (diencephalic) roof plate; MB, midbrain vesicle (approximate border with interbrain shown by dashed line); sfi, fimbrial sulcus; shb, habenular sulcus; shy, hypothalamic sulcus; sme, sulcus medullaris; smi, middle interbrain (diencephalic) sulcus; sopt, optic sulcus; sps, striatopallidal sulcus; ste, terminal sulcus; *, presumptive preoptic region of hypothalamus.

choroid epithelium and associated choroid plexus later form; the ependymal roof plate has been referred to recently as the cortical hem), and the commissural plate dorsally and rostrally (through which axons forming the hippocampal commissures and corpus callosum later cross to the other side). Also note that the presumptive HPF occupies a much larger area caudally, adjacent to the endbrain ependymal roof plate (with its fimbrial sulcus), and is quite narrow as it extends rostrally all of the way to the corticostriatal sulcus, adjacent to prefrontal and olfactory regions. As development progresses, the HPF caudal-ventral part associated with the temporal region expands greatly and takes the familiar adult HPF shape, whereas the rostral-dorsal part just medial to the cingulate, prefrontal, and olfactory regions remains as the tiny fasciola cinerea (caudally) and indusium griseum (rostrally).

Development of the adult HPF's familiar curved shape has been studied most carefully by Stensaas (20–25) in rabbits. As illustrated for rats (Fig. 4 *A–C*), presumptive hippocampal cortical neuron layers from the earliest stages are, as suggested above, simply a medial continuation of the cortical intermediate layer and cortical plate as a whole, with a slight external indentation representing the hippocampal sulcus (Fig. 4*B*). Also, from the earliest stages, the presumptive dentate gyrus lies immediately adjacent to the endbrain vesicle's medial edge, which caudally is represented by the fimbrial sulcus (Figs. 3 and 4). Then, Ammon's horn's medial edge comes next, adjacent to the dentate gyrus's lateral edge, followed by subicular areas, and finally the entorhinal area (Fig. 4).

By embryonic day 17, the hippocampal sulcus deepens to begin separating the presumptive dentate gyrus from Ammon's horn. This deepening is accompanied by relatively accelerated growth of the cortical plate domain forming the dentate gyrus, and this growth begins with neurogenesis in its deep or polymorph layer (Fig. 4*C*). The relatively accelerated dentate gyrus growth is supplemented by embryonic day 18 with the appearance of its granular layer, and with pronounced curvature of the dentate gyrus and Ammon's horn around the hippocampal sulcus (see arrows in Fig. 4 *C* and *D*). By embryonic day 21 (around parturition), pronounced dentate gyrus growth results in its characteristic C shape around the medial end of Ammon's horn field CA3, with the original continuity of the dentate gyrus granular layer and field CA3 pyramidal layer indicated by a red dashed line in Fig. 4 *E* and *F*. This red dashed line clarifies the continuity of hippocampal neuron layers starting from the embryonic cerebral cortical medial edge (red asterisk in Fig. 4 *B–F*) and progressing through the dentate gyrus, Ammon's horn, subicular areas, and entorhinal area, to the inferior temporal areas.

According to Hines (26), the hippocampal sulcus (fissure) is present in the 6- to 7-wk human neural tube, where it stretches from the endbrain ependymal roof plate's ventral tip near the temporal pole (blue dot in Fig. 3*A*), to the presumptive olfactory bulb near the frontal pole (green dot in Fig. 3*A*). In adult humans, the caudal segment of this embryonic hippocampal sulcus, between the dentate gyrus and Ammon's horn, is called the hippocampal sulcus, whereas the rostral segment, between the cingulate region dorsally and indusium griseum ventrally, is called the sulcus of corpus callosum (or callosal sulcus).

Basic Adult Structure–Function Organization. The hippocampal region's overall profile is C- or banana-shaped as viewed from the side of the brain, although for eutherian (placental) mammals (which have a corpus callosum), the amount of curvature and the relationship of the profile's dorsal end with the corpus callosum's caudal aspect varies (27) (Fig. 5*A*). Generally, the "banana's" long axis defines the hippocampal region's longitudinal axis with its two ends (Fig. 5*A*). The end near the corpus callosum is referred to as dorsal, septal (based on its proximity to the septal region's caudal end), or posterior (based on its position described

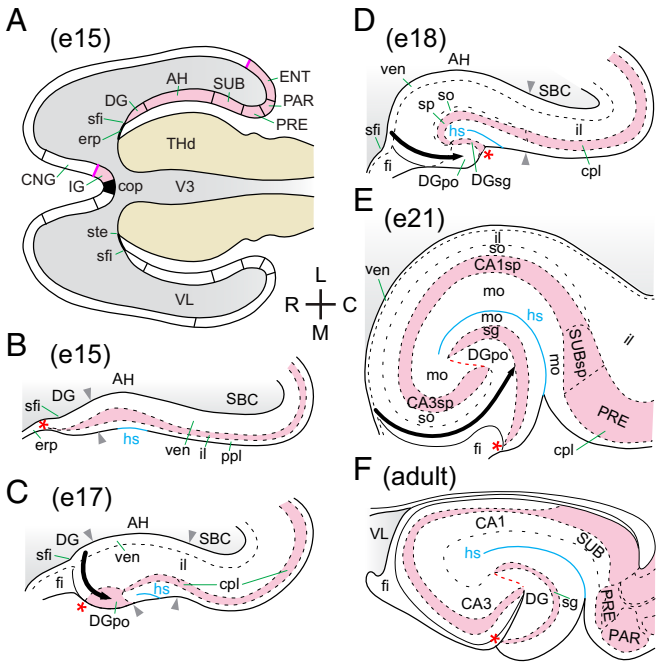

Fig. 4. HPF developmental sequence illustrated for the rat, progresses from a gently curved sheet early in endbrain development (*A*) to the convoluted cortical sheet found in adults (*F*). (*A*) A schematic horizontal section of the forebrain vesicle on embryonic day 15 (e15; approximate viewing angle shown by dashed line in Fig. 3*B*). A fate map of HPF cortical area spatial relationships is shown for the right cerebral hemisphere (pink shaded, with magenta boundary lines in *A*; compare with *B*–*F*). (*B*) The earliest stage of neurogenesis from the ventricular layer (ven) produces an intermediate layer (il) of young neurons extending laterally from the fimbrial sulcus (sfi), with an outer preplate layer (ppl). The positions of the presumptive dentate gyrus (DG), Ammon's horn (CA), and then subicular areas (SBC; subiculum, presubiculum, postsubiculum, parasubiculum) are shown relative to the fimbrial sulcus, and the first hint of the hippocampal sulcus (hs; in blue) lies superficial to a slight bulge in Ammon's horn intermediate layer. Here and in *C*–*F*, the embryologically and topologically medial edge of the HPF is indicated with a red asterisk (*). (*C*) By embryonic day 17 (e17) a cortical plate (cpl) has differentiated from the intermediate layer, dentate gyrus polymorph layer (DGpo) neurons begin a marked accumulation after generation in the ventricular layer (thick arrow, also in *D* and *E*), the hippocampal sulcus deepens, and the fimbria (fi) begins differentiation. (*D*) By embryonic day 18 (e18) the hippocampal sulcus deepens further, accompanied by the presumptive Ammon's horn curving around it; and Ammon's horn stratum oriens (so) and the dentate gyrus granular layer (DGsg) form. (*E*) Around parturition (embryonic day 21, e21) the HPF has grown considerably and the dentate gyrus has a C-shaped appearance, with its polymorph layer (DGpo) now separating the lateral end of the dentate gyrus granular layer (sg) from the medial end of the field CA3 pyramidal layer (CA3sp) (see dashed red line, also shown in *F*). (*F*) Adult configuration of the basic arrangement shown in *E* (for more details see Fig. 6). Abbreviations: C, caudal; CNG, cingulate region; cop, commissural plate; IG, indusium griseum; L, lateral; M, medial; R, rostral; for other abbreviations see Figs. 2 and 3. Parts *B*–*F* adapted with permission from ref. 38.

in human terminology), whereas the end near the distal tip of the lateral ventricle inferior horn is referred to as ventral, temporal (based on its proximity to the cerebral hemisphere's temporal pole), or anterior (based on its position described in human terminology).

The basic sequence of hippocampal cortical areas shown in Fig. 4 is displayed on the face of slices of the HPF when it is cut transversely to its longitudinal axis (creating cylindrical blocks, as obtained by slicing a banana similarly): that is, when the HPF is cut transversely to its curved longitudinal axis (Fig. 5*A*). However, HPF longitudinal axis curvature prevents the complete sequence of nine major HPF areas, from the dentate gyrus through lateral entorhinal area, from being seen in any single rodent brain transverse (coronal, frontal) section. The full sequence is observable only in a narrow strip of horizontal sections (for mouse see Fig. 6; for rat see figures 2 and 3 in ref. 28).

The HPF areal parcellation and laminar differentiation shown in Figs. 2 and 6 is based on the foundational analysis of Blackstad (29) in rat, as adapted in ref. 28. The rationale for including this particular set of adjacent cortical areas within a unitary HPF is that all of these areas are linked together by a predominantly transversely oriented series of excitatory axonal connections called the intrahippocampal circuit (28) (Fig. 5*B*). The trisynaptic circuit —from the entorhinal area to dentate gyrus to field CA3 to field CA1—is the best-known intrahippocampal circuit component (30)

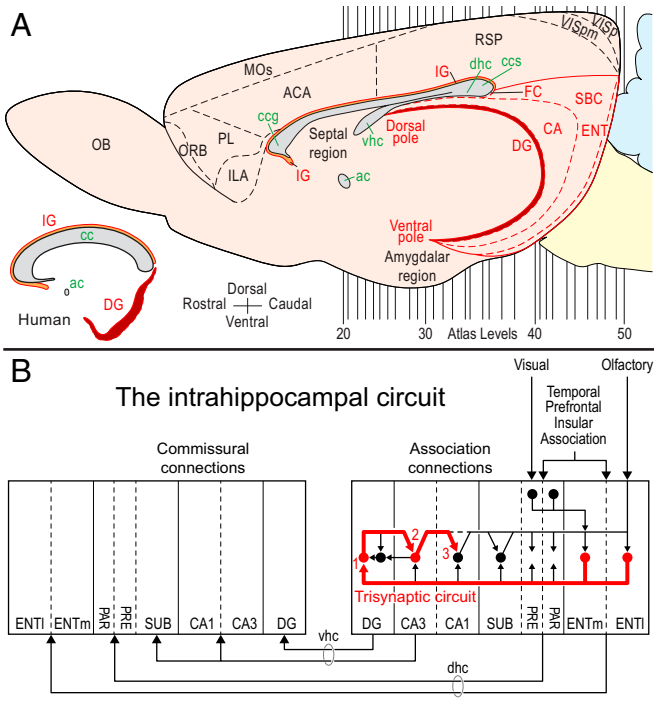

Fig. 5. (*A*) Basic HPF (red outline) C- or banana-shaped profile, viewed from the side. The rat brain's right half is shown in a schematic projection of the midsagittal (median) plane, and the C shape with its longitudinal axis are most easily appreciated by considering the dentate gyrus (dark red shading). The longitudinal axis ends are called poles, and cuts or slices transverse to the longitudinal axis show to varying degree the sequence of hippocampal cortical areas shown in Figs. 4 and 6. In different species, the dorsal pole position may vary relative to the corpus callosum caudal end, as is well-known for humans (*Inset, Lower Left*) (27); note also the indusium griseum (IG, shaded orange) location. Atlas levels (20 to 50) are from ref. 8. (*B*) Basic intrahippocampal circuit components with association (within one side) and commissural (between sides) connections between the HPF cortical areas; the intrahippocampal circuit's trisynaptic component is in red. These connections orient mainly transverse to the HPF longitudinal axis shown in *A*, but the spread of individual projecting axons varies from narrow (dentate gyrus mossy fibers to field CA3, or field CA1 to subiculum) to wide (entorhinal area to dentate gyrus or field CA3 to field CA1). This scheme is based on experimental pathway-tracing experiments in rats, where the intrahippocampal circuit's overall transverse orientation has been displayed on flatmaps; see review in ref. 28. Adapted with permission from ref. 28. Abbreviations (not in Fig. 2): ac, anterior commissure; ACA, anterior cingulate area; CA, Ammon's horn; cc, corpus callosum, ccg, corpus callosum genu; ccs, corpus callosum splenium; dhc dorsal hippocampal commissure; ILA, infralimbic area; ORB, medial orbital area; MOs, secondary somatomotor areas; OB, olfactory bulb; PL, prelimbic area; RSP, retrosplenial area; SBC, subicular complex (subiculum, presubiculum, postsubiculum, parasubiculum); vhc, ventral hippocampal commissure; VISp, primary visual area; VISpm, posteromedial visual area.

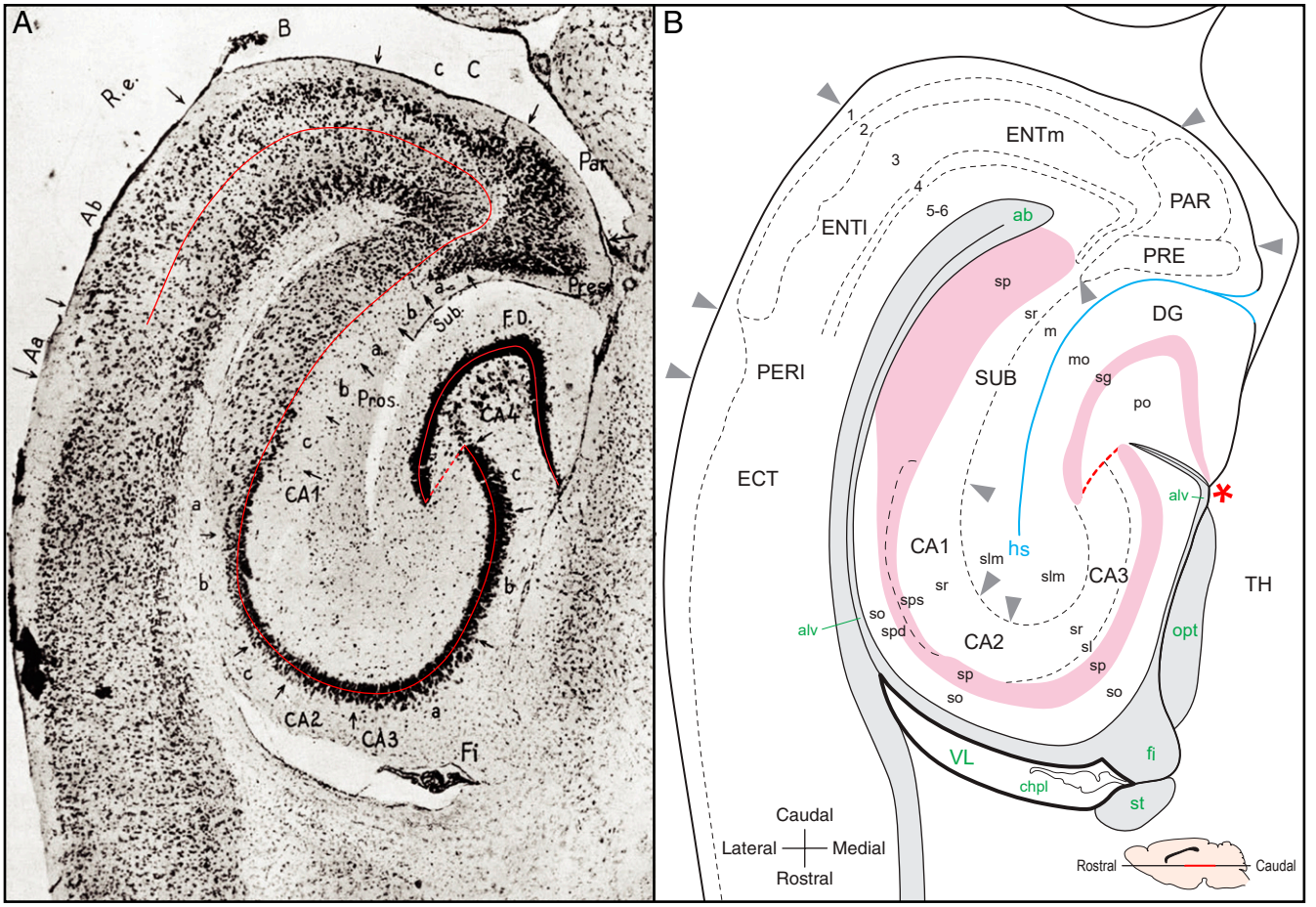

Fig. 6. Sequence of HPF cortical fields shown in a mouse forebrain horizontal section (right side, rotated 90° counterclockwise relative to Fig. 4). (*A*) The Nissl-stained section used by Lorente de Nó (17) to show his parceling of this cortical territory, with a thin red line added here to show the "surface" used for creating the rat 3D model (see *B* for layer location: dentate gyrus and Ammon's horn, middle of neuron layer; subiculum, border between pyramidal and radiatum layers; rest of retrohippocampal region, middle of layer 3). Published in Lorente de Nó, ref. 17. (*B*) A tracing of the photomicrograph in *A* to show the simplified parceling used here (Fig. 2); for horizontal section location see red line segment in the *Inset* (*Lower Right*). Layers 1 to 6 apply to lateral and medial entorhinal areas (ENTl, ENTm), parasubiculum (PAR), and presubiculum (PRE; and its dorsal segment, the postsubiculum), and do not correspond to isocortical layers 1 to 6. Layering is different for subiculum (SUB), for fields CA1 to CA3, and for dentate gyrus (DG). Lorente de Nó defined field CA2 as having large pyramidal neurons (CA2sp; as in field CA3sp), but lacking a *stratum lucidum* (sl; mossy fiber input). As in Fig. 4, the red asterisk (*) indicates the cortical mantle medial edge and the dashed red line indicates where the major neuron layers of dentate gyrus and field CA3 separate during development. Note the lateral ventricle choroid plexus (chpl) that develops (Figs. 3 and 4) from the ependymal roof plate, between the fimbrial sulcus (where fimbria, fi/Fi develops) and terminal sulcus (where terminal stria, st, develops). Abbreviations for *A*: Aa, regio perirhinalis (which Lorente de Nó included in R.e.); Ab, B, C, parts of regio entorhinalis (R.e.); CA1 a, b, c, parts of field CA1; CA3 a, b, c, parts of field CA3; CA4 (DGpo in *B*); F.D., fascia dentata; Par, parasubiculum; Pres, presubiculum; Pros. a, b, c, parts of prosubiculum; R.e, regio entorhinalis; Sub. a, b, parts of subiculum. Abbreviations for *B*: see Figs. 2–4 and: ab, angular bundle; alv, alveus; chpl, choroid plexus of lateral ventricle; ECT, ectorhinal area; opt, optic tract; PERI, perirhinal area; st, terminal stria; TH, thalamus.

(Fig. 5*B*), and has been studied extensively, especially to clarify synaptic mechanisms of long-term potentiation (31).

Topological Flattening of the HPF. A rat HPF flatmap originally was created from a physical model to plot and compare the results of anterograde pathway-tracing experiments having injections centered at different dorsal-ventral levels of the HPF longitudinal axis (5). Without a currently available physical or, better yet, computer graphics model constructed appropriately to generate quantitatively a mouse hippocampal flatmap, our solution and practical application is based on the assumption that general HPF topographic and topological features in rat and mouse are qualitatively similar. This assumption is supported by the observation that the overall HPF C-shaped profile, as judged by the dentate gyrus and its position relative to the corpus callosum, appears to be very similar in rat and mouse (Fig. 7), and quite different from the human arrangement (Fig. 5*A*). Spatial similarity between rat and mouse HPF is also indicated by similar relative longitudinal axis position of its major divisions, and by a rescaled comparison of mouse to rat for these divisions (*SI Appendix*, Fig. S1).

The method used to construct the original rat HPF flatmap is described in detail because its practical use for mapping data are exactly the same in mouse or rat, and depends on a clear understanding of how the map's graphical elements relate to the physical brain from which the data are derived. This description is also provided because it is a conceptual guide to a general, quantitative solution for the hippocampal flatmap problem in mammals, including humans.

To start, a large physical model was created using the Born method of wax-plate reconstruction (32), but with sheets of flexible foam rubber instead. For this, a 1-in-5 series of 30-μm-thick Nissl-stained transverse sections was magnified 82 times, and the major neuron layers were plotted for each section (as illustrated for a mouse horizontal section in Fig. 6*B*). Because the model's surface was to be used for flatmap construction, and because of

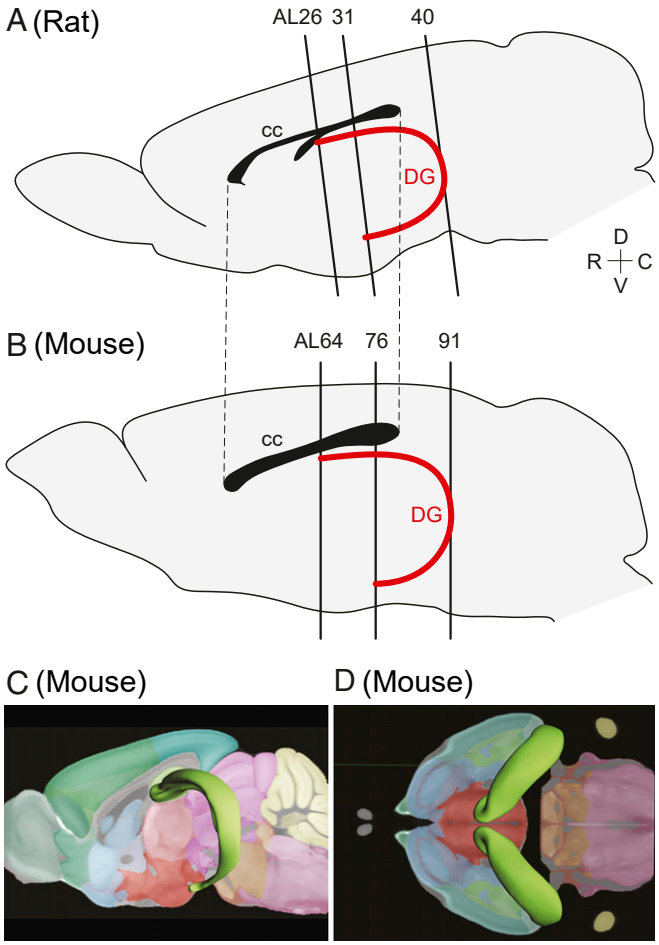

Fig. 7. Comparison in rat and mouse of the overall C shape of the HPF when viewed in profile, as illustrated for the dentate gyrus. (*A* and *B*) To a first order of approximation the profiles and their relationship to the corpus callosum (cc; black), viewed from a midsagittal perspective, are very similar, and quite different from human (Fig. 5*A*). Data from ref. 8 and 34. For each atlas, the rostral tip (mouse AL64, rat AL26), caudal tip (mouse AL91, rat AL40), and ventral tip (mouse AL76, rat AL31) was determined, and the overall C shape (red line) was drawn using these three points, with intervening ALs used as a guide. For comparison, the brain outlines were scaled to approximately the same length, then the rat brain outline was rotated to align the corpus callosum with the mouse corpus callosum, and finally the rostral-dorsal tips of the dentate gyrus in both brains were aligned. Note the remarkable correspondence between the scaled lengths of the corpus callosum (which are at the same angle) in the two brains (indicated by vertical dashed lines; also see *SI Appendix*, Fig. S1). It is also important to note that this analysis suggests the HPF was cut at a different angle in the rat and mouse brain atlases used for these reconstructions. (*C* and *D*) Three-dimensional surface models of the mouse dentate gyrus (green) viewed from the lateral (*C*) or dorsal (*D*) side of the brain. The dorsal view (*D*) shows that the right and left dentate gyrus together form an approximately right angle, each 45° relative to the median plane (longitudinal axis). For orientation, a sagittal (*C*) and horizontal (*D*) brain section is shown behind the surface models. (*C* and *D*) from the average mouse brain in ref. 35. Abbreviations: C, caudal; D, dorsal; R, rostral; V, ventral.

extreme curvature in parts of the HPF (especially in presubiculum and parasubiculum; see below in this section), an approximate midpoint in cortical thickness was chosen to represent the HPF model's surface (see red line in Fig. 6*A*).

The magnified HPF outlines, with boundaries between each cortical area, were then transferred onto foam rubber sheets with a thickness scaled to the distance between histological sections (5 × 30 μm), the hippocampal outline on each sheet was cut out, and the resulting 39 foam rubber pieces were aligned and glued together to form the physical model (with boundaries between cortical areas marked). Then, a piece of clear polyethylene film was stretch-wrapped carefully over each individually marked cortical area, and the boundaries with adjacent areas were traced onto the film, along with the location of each boundary between adjacent foam rubber sheets (representing the width of each of the 1-in-5 series of histological sections).

The tracings for each hippocampal cortical area were then placed side by side and aligned, using as guides the continuity between histological section lines and areal borders to produce a complete unfolded or flatmap of the HPF. The two graphical elements of the flatmap are thus 1) the set of boundary lines between all HPF cortical areas, and 2) the overlapping set of contour lines representing the location of transverse sections through the HPF.

This procedure does not produce a truly accurate representation of each cortical area's surface area because it is impossible to apply sheets of polyethylene film to the model's curved surface without some wrinkling. However, the procedure does provide a reasonably accurate qualitative flatmap representation for the convoluted but essentially sheet-like HPF structure.

Later, the rat hippocampal flatmap was revised and updated (Fig. 8*B*) (7). First, the dentate gyrus was realigned so that its medial, free edge (red asterisks in Figs. 4 and 6) forms the map's medial (rather than the original lateral) edge, and second, the approximate location of Atlas levels (ALs) from our rat brain atlas (33) were added.

The updated rat HPF flatmap (Fig. 8*B*) was used as a template for creating a mouse HPF flatmap of ALs using the transverse series of sections in the *Allen Reference Atlas* version 1 (34) (Fig. 8*A*). ALs 64 to 104 contain the HPF, so the *Allen Reference Atlas* has almost twice as many sections covering the HPF compared with the rat brain reference atlas (41 sections versus 23). The sections between ALs 64 to 104 in the mouse brain reference atlas are mostly spaced evenly at 100-μm intervals (1-in-4 series of 25-μm-thick Nissl-stained sections), although 10 ALs diverge from this even spacing, ranging from an interval of 75 to 225 μm from the rostrally preceding section.

Aligning the set of 41 mouse AL contours was done manually, as described for the rat HPF (Fig. 8*B*). The rat contour map's overall pattern was used as a nominal template for constructing the mouse contour map, anchored to the HPF flatmap (Fig. 8*A*; see Dataset S1 for a computer graphics file designed for mapping) using boundary relationships and obvious fiducial points. The latter included the dentate gyrus rostral-dorsal tip (AL64), dentate gyrus caudal tip (AL91), dentate gyrus-CA3 ventral tip (AL76), lateral entorhinal area rostral tip (AL69), and cerebral cortex occipital pole (AL104). For orientation, compare the "X"-shape of mouse AL80 (Fig. 8*A*) with its counterpart in the rat flatmap (AL35 in Fig. 8*B*). For a mouse brain section of a comparable level cut in roughly the same plane as the rat used for the flatmap, see the right side of *SI Appendix*, Fig. S2*B*.

Based on Nissl-stained AL sections, rat and mouse HPF parceling is virtually identical in rat Brain Maps 4 (8) and the *Allen Reference Atlas* version 1 (34), whereas HPF parceling in the *Allen Reference Atlas* version 3 remains incomplete at this time (35). The only serious ambiguity between Brain Maps 4 and the original *Allen Reference Atlas* concerns the border between ventral parts of field CA1 and the subiculum, which is not indicated consistently in the latter. Classically, field CA1 and subiculum (with its prosubiculum) are distinguished most clearly by the presence of *stratum oriens* in field CA1 and its absence in the subiculum (rat Brain Maps 4, ALs 32 to 40). In the *Allen Reference Atlas* version 1, the ventral subiculum's rostral tip is indicated correctly on AL79, and caudally on ALs 83 to 91, but on ALs 80 to 82 the ventral subiculum's ventral tip is included

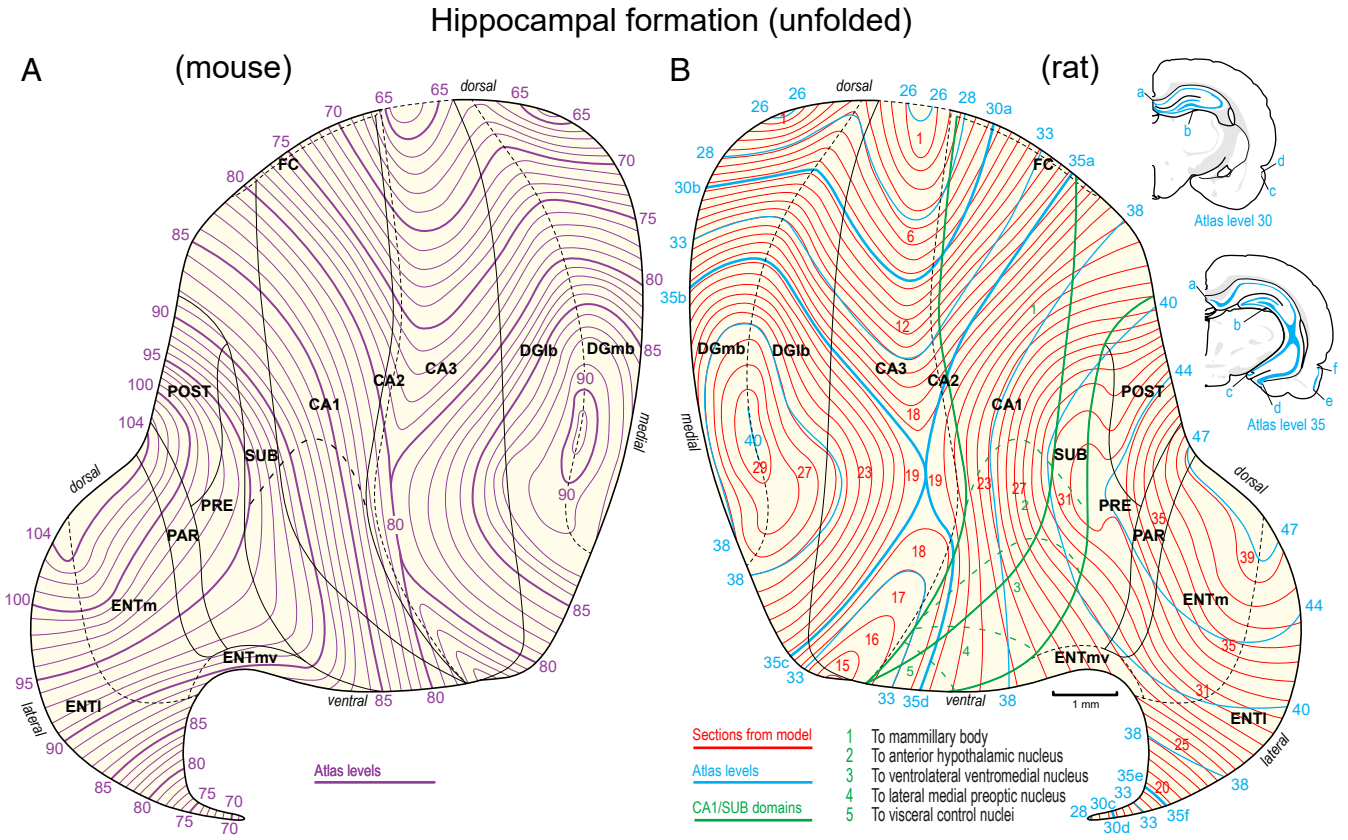

Fig. 8. Mouse and rat hippocampal flatmaps. (*A*) Mouse HPF flatmap that is identical in outline to the rat HPF flatmap (*B*) that was generated from a physical surface model but flipped along the vertical axis and with ALs 64 to 104 (numbers and purple contour lines) delineated from the *Allen Reference Atlas* version 1 (34). For parceling, the *Allen Reference Atlas* version 1 (34) was used because hippocampal delineations are more complete than in the current version 3 (35). Anchoring the AL contour map was done manually as described for rat in the text (and this legend). (*B*) Rat HPF flatmap showing the disposition of histological transverse sections (30-μm thick, 1-in-5; red contour lines) from a physical surface model (5), and of ALs (blue contour lines) from ref. 39. Atlas Levels 30 and 35 (*Upper Right*) show how hippocampal cortical areas transform from the ALs (transverse sections) onto the flatmap by using the same points, a to f, on the ALs and flatmap. The terminology for the rat differs slightly from that used here: dentate gyrus medial blade (DGmb) and lateral blade (DGlb) are not recognized, and a medial entorhinal area ventral zone (ENTmv) is not distinguished from the medial entorhinal area (ENTm) (Fig. 2). The field CA3 dorsal end is without border because its rostral tip is hemispherical and was cut for flattening (see figure 1 in ref. 45). The top thin green dashed line across the middle of field CA1 and subiculum (between domains 1 and 2) is an operational border between dorsal and ventral parts of these adjacent cortical areas (see ref. 7). The border between postsubiculum and presubiculum is adjusted here to conform better with histological analysis. For abbreviations, see Fig. 2. Adapted with permission from ref. 7, where CA1/SUB domains 1 to 5 (delimited by dashed green lines) are explained.

incorrectly in ventral CA1 (compare with rat Brain Maps 4, ALs 32 to 40). In the *Allen Reference Atlas* version 3, the ventral subiculum's ventral end is delineated "hippocampo-amygdalar transition zone, HATA" on ALs 81 to 93.

Distortions, Contour Patterns, and Practical Mapping. Distortions are inevitable when mapping from a curved surface to a flat surface while, as here, preserving accurate boundary relationships (36). Thus, at least qualitatively, the hippocampal flatmap accurately transforms topologically the physical model's surface features: The flatmap shows boundary relationships clearly between the various hippocampal cortical areas, and the relative surface area of those cortical areas. It is obvious that the HPF consists of a series of longitudinal cortical strips (with a dorsal and a ventral end), arranged from medial (dentate gyrus) to lateral (lateral entorhinal area) (Fig. 8).

The flatmap delineation and spacing of contour lines representing HPF division boundaries and histological sections reflects the folding exhibited by the adult HPF (Figs. 5 and 6), which arises developmentally from a nonfolded cortical sheet (Figs. 3 and 4). This folding explains the uneven spacing between section contour lines on the HPF flatmap: The spacing of adjacent section contour lines corresponds to the relative change in surface area curvature between the adjacent transverse sections for each HPF division; the greater the change in curvature, the more widely spaced the contour lines (Fig. 9 *A*–*C*). It is also important to consider which cortical "surface" to represent in the flatmap model. Because of extreme curvature, for example, in the presubiculum and parasubiculum, a line drawn roughly halfway through the depth of the cortex was used for the model because such a line approximates an average surface area (Figs. 6*A* and 9*D*).

The approach for transferring histological data to the hippocampal flatmap is shown in Fig. 8*B* for two sections, ALs 30 and 35 (Fig. 8 *B*, *Upper Right*). The HPF parts (colored blue in Fig. 8*B*) in these two ALs are also shown on the flatmap as blue lines, and the orientation of corresponding blue lines in the ALs and on the flatmap is shown by corresponding blue letters a–f. Thus, far, data from histological sections have been transferred to the flatmap qualitatively (but see below). As mentioned above, examples of histological data displayed on the rat hippocampal flatmap have been published previously (3, 5, 7, 9, 10, 37). In principle, the manual transfer of data from any transversely evenly spaced sectioned brain involves comparing the number of

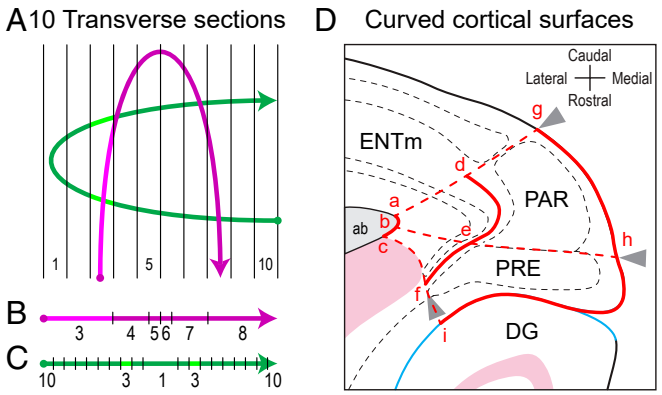

Fig. 9. Effects of curvature on the hippocampal flatmap. (*A*) Two hypothetical curves (green and purple) with the same shape but orthogonal orientations, both transected by 10 evenly spaced sections. (*B* and *C*) Demonstration of how each segment of each curve contained within the 10 sections shown in *A* map onto a straight line when the proportional path length of each curve segment is preserved, from the line's origin (indicated by a circle) to its end (indicated by an arrowhead). Note two distinct spacing patterns result from differences in curve orientation and consequent difference in path length of each segment between sections (highlighted for the segments traversing section 3). (*D*) When curved, a cortical field's "surface area" in the physical model depends on whether the outer surface, inner surface, or an intermediate demarcation is used. The presubiculum and parasubiculum present extreme examples (the underlying map is from Fig. 6*B*). The presubiculum (PRE) outer surface is relatively long and oddly shaped (h, i), whereas the inner surface (b, c; formed by the angular bundle, ab) is relatively very short with a shallow curve. For flatmap construction, an intermediate line through the middle of layer 3 was used (e, f). The parasubiculum (PAR), with its outer surface (g, h), inner surface (a, b), and intermediate line (d, e), provides a similar, less extreme example. The intermediate line used for the entire HPF is shown in red in Fig. 6*A*. Abbreviations: DG, dentate gyrus; ENTm, medial entorhinal area.

histological sections in that brain with the number of sections in the flatmap, and then manually interpolating data transfer onto the set of reference section contours on the flatmap using 1) cortical area boundary conditions and 2) obvious fiducial points, such as the rostral and caudal tips of the dentate gyrus and lateral entorhinal area.

Flattening the Entire Cerebral Cortex. Once a rat HPF flatmap was achieved, it was relatively easy to generate a flatmap of the entire rat cerebral cortex. The basic approach included starting with a rat cerebral cortex fatemap from the earliest stages of endbrain development (as in Fig. 3), preserving all cortical gray matter region boundary conditions present in adults, and sizing the area for each cortical region on the flatmap in proportion to qualitative estimates of the actual surface area for each cortical region (for details, see refs. 6 and 38).

The cortical flatmap's overall shape, which was included in a flatmap of the entire central nervous system (CNS) (6, 38) (Fig. 10*C*), aligns with the spoon-shape of the neural plate, the earliest stage of nervous system development, where the primordium of the brain (the spoon's bowl) and spinal cord (the spoon's handle) is topologically a flat sheet (before invaginating longitudinally to form the neural tube). To conform with the shape of this cortical map, the original HPF flatmap generated from the physical model was warped manually while preserving boundary conditions and relative surface areas of all hippocampal cortical regions (Fig. 10*A*). Thus, the HPF flatmap underwent two topological transformations, from the physical model, and then to the cortical part of the CNS flatmap's predetermined shape. The latter HPF flatmap configuration was later updated with a contour map of ALs 27 to 48 (Fig. 10*B*) (39).

In this cortical flatmap the HPF dorsal and ventral ends remain obvious, along with the sequential arrangement of its nine major longitudinally oriented parts, from the dentate gyrus to lateral entorhinal area (compare Figs. 8*B* and 10). Clearly, however, there is more distortion than in the first configuration. For example, the dentate gyrus, along the relatively short cerebral cortex medial edge, is stretched like Antarctica on a common rectangular Earth map.

After the first version of the mouse HPF flatmap was generated (Fig. 8*A*), a second topological transform using the rat cortical parcellation as a template was then performed manually (Fig. 11). The approach used for warping the rat AL contour map from the physical model (Fig. 8*B*) to the whole cortex outline (Fig. 10*B*) was also used for the mouse. Each HPF flatmap configuration (first from the physical model, and then one embedded in a complete cortical map that in turn is embedded in a CNS map) provides a different graphical representation that may be useful for comparative purposes.

A HPF Coordinate System. The longitudinal and transverse axes of the HPF, and of all its constituent areas, suggests that once the cortical sheet is unfolded and flattened, it should be easy to create an intrahippocampal coordinate system analogous to the Earth's longitude and latitude. One conceptual way to do this is shown in Fig. 12. Starting with the cortical flatmap (Figs. 10 and 11), hippocampal area borders serve as an initial series of longitudinal lines, and a series of transverse lines is then generated with arbitrary but convenient spacing (Fig. 12*A*). This procedure generates a coordinate system, but perhaps a more intuitively useful coordinate system can be generated by warping topologically the flatmap to "square off" the HPF's four corners: The dorsal and ventral ends of the dentate gyrus and lateral entorhinal area (Fig. 12*B*). Then, a series of equally spaced longitudinal and transverse lines is drawn, and a coordinate system origin is defined, for this example, at the dentate gyrus dorsal tip. This constitutes a third-stage topological transformation of original spatial relationships in the brain itself.

The dentate gyrus dorsal tip is at the map's topological dorsomedial corner (0, 0) (Fig. 12*B*), whereas the lateral entorhinal area dorsal tip is at the dorsolateral corner (arbitrarily 0, 1), the dentate gyrus ventral tip is at the ventromedial corner (0, 1), and the lateral entorhinal area ventral tip is at the ventrolateral corner (1, 1). Any point on the map is thus described by two unique coordinate values.

Finally, if an AL contour map (Figs. 10 and 11) is warped along with the underlying cortex flatmap (Fig. 12*A*) to the squared-off flatmap (Fig. 12*B*), then the flatmap coordinate system can be transferred to the hippocampal structures in the transverse brain sections forming the reference atlas. This provides a systematic way to transfer data in experimental sections (assuming they are accurately aligned with the reference atlas) to the HPF flatmap representation using the same coordinate system.

In principle, any convenient coordinate system can be mapped onto the "squared off" flatmap coordinate system shown in Fig. 12*B*. One example might be the Allen Mouse Common Coordinate Framework version 3 with its average brain in 3D space (35).

Proof-of-Concept Examples. As exemplars, the two mouse HPF flatmap configurations were used to display the general course of mossy fiber projections arising from different sites along the dentate gyrus longitudinal axis. For this, the results of anterograde rAVV pathway-tracer experiments in the *Allen Mouse Brain Connectivity Atlas* (40) were plotted. The most dorsal and most ventral injections in the *Allen Mouse Brain Connectivity Atlas* were analyzed, along with three injections in between (Fig. 13). The results clearly suggest that during most of their course

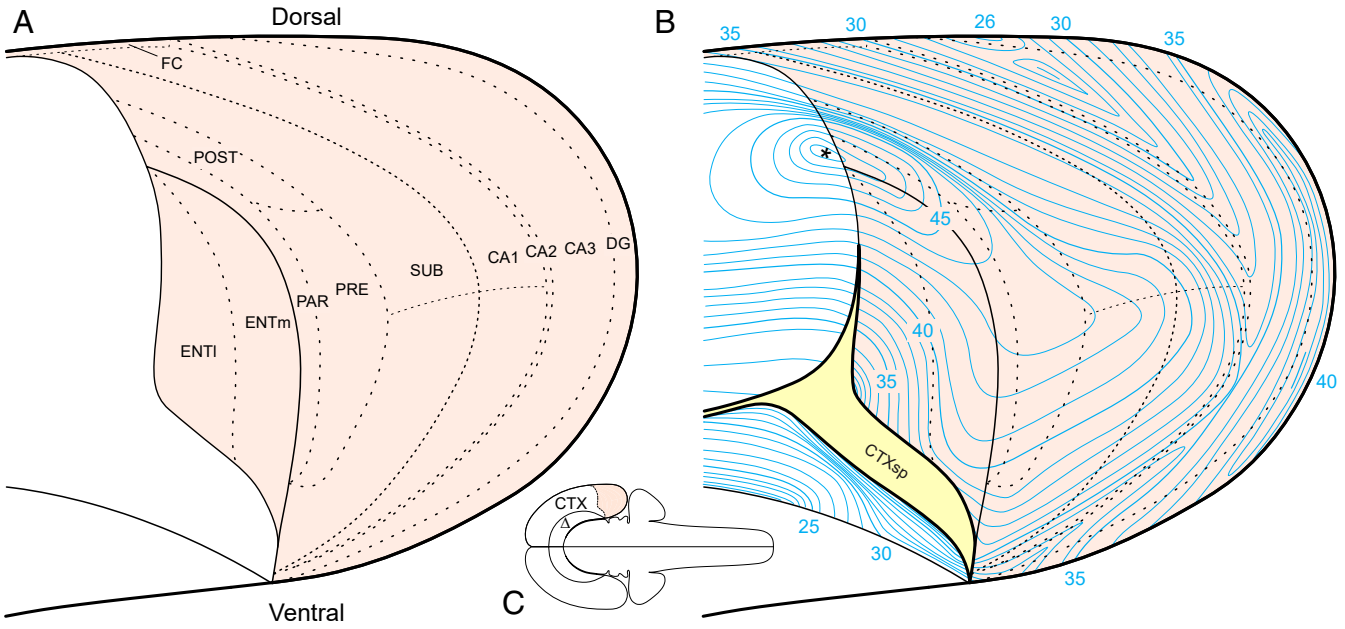

Fig. 10. Rat hippocampal flatmap generated from the physical surface model (Fig. 8*B*) warped onto the predetermined shape of the cerebral cortex within a flatmap of the entire CNS. (*A*) HPF cortical area arrangement, with dentate gyrus along the map's medial edge (see Figs. 3 and 4). Once the dentate gyrus is thus positioned on the flatmap, there is only a single way to place the other HPF parts and maintain correct boundary relationships. For simplicity, the rest of the cortical map is not shown. This map was used as a template for the corresponding mouse HPF flatmap (Fig. 11). The thin dashed line across field CA1 and adjacent subiculum indicates an operational border between dorsal and ventral parts of these cortical areas (see green dashed line between domains 1 and 2 in Fig. 8*B*). (*B*) A mapping of ALs (8) onto the cortical flatmap (*A*). This topological transformation was accomplished manually by starting with the contour pattern in the map from the physical model (Fig. 8*B*). Then the AL map was anchored to the cortical flatmap (*A*) using boundary relationships and obvious fiducial points: Dentate gyrus rostral-dorsal tip (AL26), dentate gyrus caudal tip (AL40), dentate gyrus ventral tip (AL31), lateral entorhinal area rostral tip (AL30), and cortex occipital pole (AL49). For orientation, compare AL35, with its "X"-shape, here and in the physical model flatmap (Fig. 8*B*, including *Inset* at *Upper Right*). The yellow part interrupting the AL contour map at *Lower Left* represents the cortical subplate (CTXsp), nested in the main map (representing the cortical plate) and thus interrupting the contour map. The asterisk (*) indicates the cerebral cortical occipital pole. (*C*) Hippocampal flatmap location (light pink area) on *Right* side of cerebral cortex (CTX) part of entire CNS flatmap; the cerebral nuclei are indicated by a triangle (Δ). For abbreviations see Fig. 2. Figure adapted with permission from ref. 8.

through field CA3, mossy fibers maintain a very strict parallel (transverse) orientation, until they approach field CA2, which they avoid by coursing caudally for a short distance and overlapping in Lorente de Nó's (17) subfield CA3a (Fig. 6), at least for subfield CA3a's dorsal half (dentate gyrus injections centered more ventrally are not available). These results suggest that mossy fibers from adjacent dorsoventral sites overlap very little in subfields CA3c and CA3b (Fig. 6), whereas mossy fibers overlap considerably in subfield CA3a as they course ventrally for a relatively short distance. Note how each flatmap configuration has different spatial distortions that will differently affect the graphical representation of mapped data.

To complement the connectional data, the Purkinje cell protein 4 (Pcp4) gene-expression pattern was also displayed on the flatmaps (Fig. 13). It has been suggested that Pcp4 provides a "molecularly defined" field CA2 (41), which does not correspond exactly to Lorente de Nó's (17) histologically defined field CA2 (Fig. 6), characterized by large pyramidal neurons (like those in field CA3) without a mossy fiber input (a *stratum lucidum*). The Pcp4 expression pattern was obtained from ref. 42, and along the longitudinal axis it appears that Pcp4 is expressed heavily in the histologically defined field CA2, in a narrow zone of scattered neurons in the immediately adjacent field CA1, and in a broader, tapering band of neurons in subfield CA3a (Fig. 14). It remains to be shown whether neurons in these three zones of the molecularly defined field CA2 have different or similar sets of input and output connections.

Brains with pathway-tracer injections, gene-expression markers, or other histochemical procedures are almost never cut in exactly the same plane of section as a 2D atlas, so there are inevitable right–left, and dorsal-ventral, asymmetries that cannot be entirely eliminated by warping onto a single nearest available AL (43). When this mismatch occurs, a final step of manual alignment between individual experimental sections and multiple ALs or a flatmap is necessary. An example from the dataset used to plot the Pcp4 intrahippocampal expression pattern (Fig. 13) is shown in *SI Appendix*, Fig. S2 *A* and *B*. It is also important to note that *Allen Reference Atlas* version 1 (34) was used here for flatmap construction and data plotting; the HPF is not yet adequately parceled in version 3 (*SI Appendix*, Fig. S2 *C* and *D*).

Requirements for a Quantitative Flatmap. A practical solution for generating quantitatively a flatmap of the HPF, or of the entire cerebral cortex, involves creating a computer graphics surface model that 1) has a coordinate system derived from the parent reference brain, 2) can be warped topologically from 3D to 2D, and 3) can represent accurately spatial data from experimental brains. A necessary starting point for this goal is a high-resolution 3D computer graphics brain model with all recognizable gray matter regions (including subregions and layers) and white matter tracts parceled accurately. If constructed properly, this brain model could be used to generate any surface model desired (for example, based on the red line in Fig. 6*A*), but equally importantly, it could be sliced in any plane, specifically in the plane of an experimental brain, thus eliminating the "plane-of-section error" associated with matching histological sections with standard 2D ALs (43) (*SI Appendix*, Fig. S2). It seems reasonable to suggest that the most useful 3D brain models will combine voxel-based and vector-based graphics (see ref. 44).

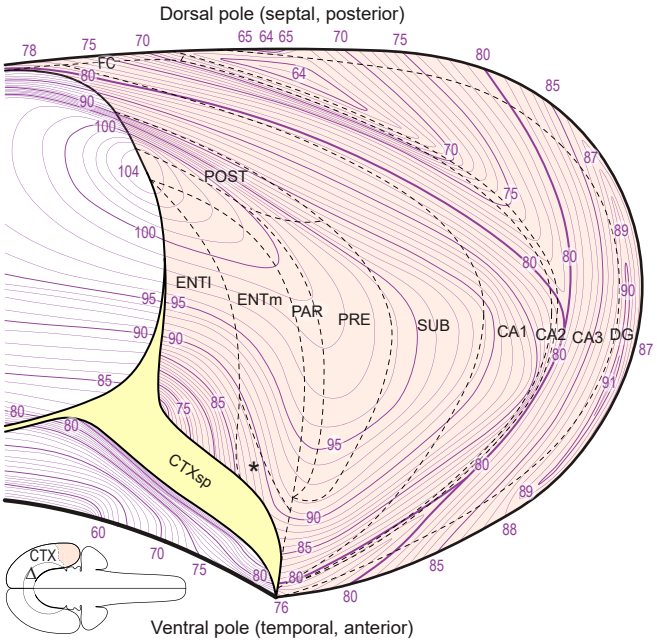

Fig. 11. Mouse HPF flatmap with AL contours (numbered purple lines) in the context of a complete cerebral cortical flatmap (for orientation see *Inset*, *Lower Left*, and Fig. 10*C*). HPF parceling (light red background) is the same as that for rat (Fig. 10*A*) and ALs (from ref. 34) were arranged as described in the text and Fig. 10*B*. The asterisk (*) indicates the medial entorhinal area ventral zone; the yellow area (*Lower Left*) represents the nested cerebral cortical subplate (CTXsp) that interrupts the AL contour map; the cerebral cortical occipital pole is represented on AL104. For abbreviations, see Fig. 2.

Discussion

Mapping is an interesting exercise, and for the present application, two cartographic principles are especially relevant (36). First, all maps are by definition simplified representations of physical reality; and second, spatial distortion is inevitable when transforming a curved surface to a flat surface, such that only one of the fundamental spatial attributes of area, shape, and distance can be represented undistorted, resulting in equivalent (equal area), conformal (equal shape), or equidistant maps, or a combinatorial compromise of these. The unfolded HPF map here is in principle an equivalent map, so cortical area shapes, and distances between physical points, are distorted. Also, maps from curved to flat surfaces can have cuts to reduce distortion (gore maps), or maps can be flattened without cuts but with more distortion (continuous maps); gore maps have the disadvantage that adjacent points near cuts can be widely separated when the map is flattened. The HPF flatmap is mostly a continuous map, although the field CA3's dorsal tip was cut (Fig. 8) because it is hemispherical (see figure 1 in ref. 45).

Cortical flatmaps are useful for simple topological comparisons of injection, stimulation, and recording sites; circuit connectional patterns; molecular expression patterns; and other data. However, it is important to recognize that whereas topological relationships are preserved, shapes and distances in our HPF equivalent flatmaps are distorted, sometimes dramatically, depending on flatmap design (compare Fig. 13 *A* and *B*). It is also apparent that these surface flatmaps cannot represent cortical laminar information; separate flatmaps for individual layers are required, although superimposable layers can be created using graphical design software (such as Adobe Illustrator) that enables separable layering.

Unless experimental brains are cut in exactly the same plane as the 2D atlas used here (34), manual adjustments in transferring data patterns to the flatmaps are necessary. This requirement will probably be largely eliminated when high-resolution 3D brain models (physical and atlas) become available, because they can be

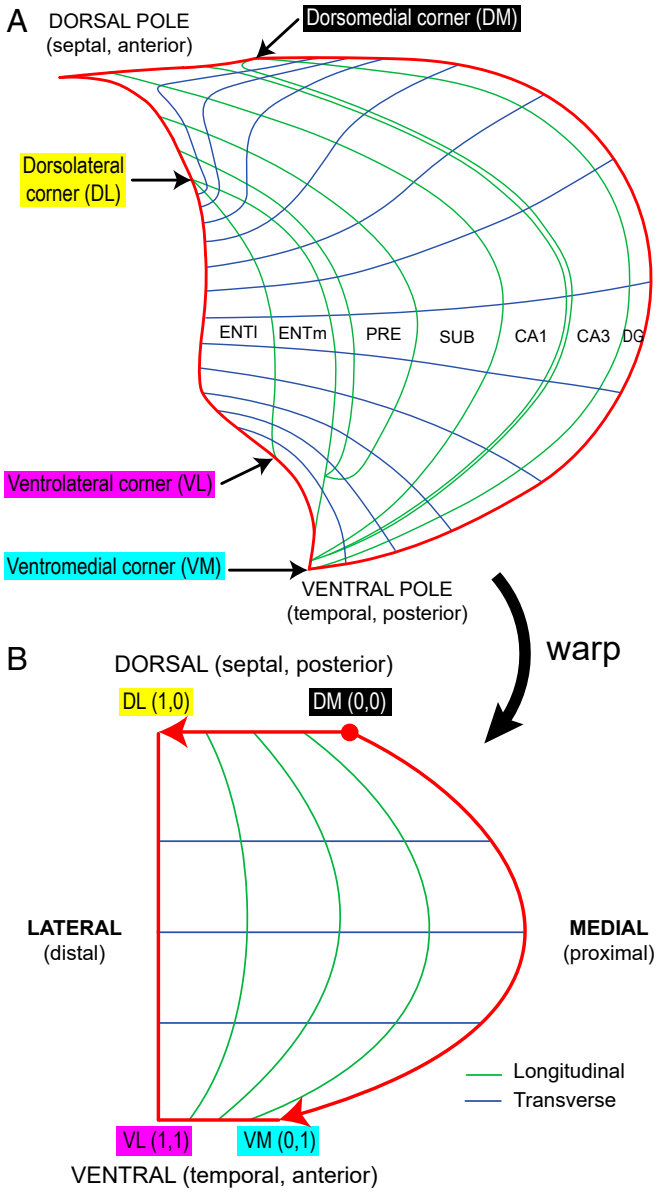

Fig. 12. Creating an intrahippocampal coordinate system for the flatmap and histological sections. (*A*) In the most straightforward approach, borders between hippocampal cortical areas (see Fig. 10*A*) serve as longitudinal grid lines (green), and lines drawn transversely (blue) at arbitrary intervals can serve as a roughly orthogonal set of grid lines. The HPF's four "corners" and its two poles are also shown. (*B*) A more intuitive flatmap coordinate system is produced by creating more obvious flatmap corners with topological warping, by drawing an evenly spaced coordinate grid, and by defining a coordinate system origin (0, 0). Background highlights (cyan, magenta, yellow, black) show point/corner correspondence in *A* and *B*. The directions (dorsal-ventral, medial-lateral) derive from topological spatial relationships established early in embryogenesis (Figs. 3 and 4), and then highly distorted by folding (Fig. 6). If an AL contour map (Figs. 10 and 11) is included in *A*, then the coordinate systems in *A* or *B* are transferred to reference ALs, and the coordinate systems are applied to experimental histological sections accurately aligned to the reference atlas. For abbreviations, see Fig. 2.

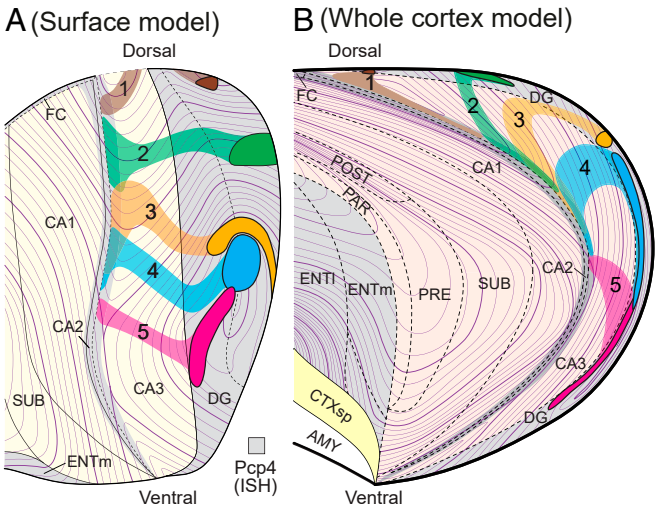

Fig. 13. Mapping axonal connections and gene expression patterns on mouse HFP flatmaps. (*A* and *B*) Five rAAV pathway-tracing experiments (1 to 5) with injection sites (dark colored blobs) involving dentate gyrus and labeled axons (specifically, just mossy fibers; lighter colored strips) extending through field CA3 in essentially parallel bundles until approaching field CA2, which they do not enter, but instead appear to curve sharply and extend ventrally for a short distance along the medial edge of field CA2 (in Lorente de Nó's subfield CA3a; see Fig. 6), where mossy fibers from adjacent DG zones appear to overlap. The Pcp4 gene expression pattern is also mapped for the HPF (gray zones) based on in situ hybridization. Note 3 longitudinal strips of apparently relatively high expression: dentate gyrus, in and immediately surrounding field CA2 (see Fig. 14), and medial and lateral entorhinal areas. Pathway-tracing experiments from ref. 40: Injection 1 is 272970039-DG; injection 2 is 114399244-DG; injection 3 is 293788700-DG; injection 4 is 293011759-DG; injection 5 is 182029174-DG. In situ hybridization data from ref. 42: Pcp4 Experiments 772 (primary), 79912613 (confirmatory). Abbreviations: AMY, amygdalar region; CTXsp, cortical subplate; for other abbreviations see Fig. 2.

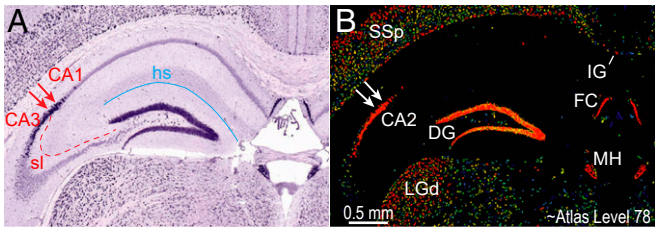

Fig. 14. Spatial distribution of Pcp4 gene expression in mouse hippocampus. (*A*) Photomicrograph of a transverse histological section with in situ hybridization for Pcp4 expression, and a Nissl counterstain partly obscuring the hybridization pattern. Magnification scale and arrows are the same as in *B*. (*B*) Pcp4 expression pattern for the section in *A*, with Nissl stain removed and hybridization signal pseudocolored for relative density (red densest). Note especially the band of hybridization in classically defined field CA2 (between two arrows), and adjacent zones of fields CA1 and CA3 (see Fig. 6). Abbreviations not in Fig. 2: hs, hippocampal sulcus; LGd, dorsal lateral geniculate nucleus; MH, medial habenula; sl, stratum lucidum; SSp, primary somatosensory area. From Pcp4 experiment 772 in ref. 42.

sliced in the same plane as an experimental brain, making atlas registration and data transfer much more accurate, combined with the development of quantitative intrahippocampal coordinate systems. It will then also be possible to determine whether differences in AL contour maps are due to biological (for example, species, strain, or sex) or methodological (for example, plane of section) differences, or a combination.

The development of high-resolution 3D brain models (with intrinsic atlases) will also be important for quantitative interspecies comparisons. For practical reasons, the mouse flatmaps described here are derived from rat flatmaps under the reasonable assumption that HPF structure is qualitatively similar in rat and mouse, but this cannot be true quantitatively. Therefore, quantitative models will produce quantitative flatmaps, allowing informative interspecies comparisons. For example, the brief analysis here of dentate gyrus to field CA3 mossy fiber system topology suggests that the distal ends of mossy fibers (in subfield CA3a, adjacent to field CA2) overlap considerably (Fig. 13), at least dorsally. This projection was first analyzed on a rat flatmap (see figure 6 in ref. 5) with the autoradiographic pathway-tracing method, and a very similar pattern of overlap was detected for field CA3 dorsal half, but not ventral half. Whether this pattern is also present in mouse can be determined when dentate gyrus ventral injections become available.

The development of a general quantitative solution to the HPF flatmap problem would also be valuable for creating human and nonhuman primate versions. A continuous, equivalent flatmap exists for adult human cerebral cortex parceled according to Brodmann (46), but no attempt has been made to produce an atlas contour map of the HPF, which displays an exceptionally complex geometry, especially ventrally (anteriorly in human), where it forms the uncus (47).

Data Availability. All relevant material is contained within the article.

1. L. R. Squire, L. Genzel, J. T. Wixted, J.T. Morris, Memory consolidation. *Cold Spring Harb. Perspect. Biol.* **7**, a021766 (2015).
2. E. I. Moser, M.-B. Moser, B. L. McNaughton, Spatial representation in the hippocampal formation: A history. *Nat. Neurosci.* **20**, 1448–1464 (2017).
3. P. Y. Risold, L. W. Swanson, Structural evidence for functional domains in the rat hippocampus. *Science* **272**, 1484–1486 (1996).
4. M. S. Fanselow, H.-W. Dong, Are the dorsal and ventral hippocampus functionally distinct structures? *Neuron* **65**, 7–19 (2010).
5. L. W. Swanson, J. M. Wyss, W. M. Cowan, An autoradiographic study of the organization of intrahippocampal association pathways in the rat. *J. Comp. Neurol.* **181**, 681–715 (1978).
6. L. W. Swanson, *Brain Maps: Structure of the Rat Brain* (Elsevier, Amsterdam, 1992).
7. G. D. Petrovich, N. S. Canteras, L. W. Swanson, Combinatorial amygdalar inputs to hippocampal domains and hypothalamic behavior systems. *Brain Res. Brain Res. Rev.* **38**, 247–289 (2001).
8. L. W. Swanson, Brain maps 4.0-Structure of the rat brain: An open access atlas with global nervous system nomenclature ontology and flatmaps. *J. Comp. Neurol.* **526**, 935–943 (2018).
9. J. M. Wyss, An autoradiographic study of the efferent connections of the entorhinal cortex in the rat. *J. Comp. Neurol.* **199**, 495–512 (1981).
10. L. A. Cenquizca, L. W. Swanson, Spatial organization of direct hippocampal field CA1 axonal projections to the rest of the cerebral cortex. *Brain Res. Brain Res. Rev.* **56**, 1–26 (2007).
11. J. W. Tukey, *Exploratory Data Analysis* (Addison-Wesley, Reading, MA, 1977).
12. G. C. Aranzi, *De Humano Foetu Liber Tertio Editus, ac Recognitus. Ejusdem Anatomicarum Observationum Liber ac De Tumoribus Secundum Locos Affectos Liber nunc Primum Editi* (Brechtanum, Venice, 1587).
13. F. Vicq d'Azyr, *Traité d'Anatomie et de Physiologie, avec des Planches Coloriées Représentant au Naturel les Divers Organes de l'Homme et des Animaux, Tome premier* (Didot, Paris, 1786).
14. C. Golgi, M. Bentivoglio, L. Swanson, On the fine structure of the *pes Hippocampi major* (with *plates XIII-XXIII*). 1886, *Brain Res. Bull.* **54**, 461–483 (2001).
15. S. R. Cajal, *Histologie du Système Nerveux de l'Homme et des Vertébrés*, Translated by L. Azoulay (Maloine, Paris, 1909–1911), vol. 2. See English translation by N. Swanson, L. W. Swanson, *Histology of the Nervous System of Man and Vertebrates* by S. Ramón y Cajal (Oxford University Press, New York, 1995), vol. 2.
16. R. Lorente de Nó, Studies on the structure of the cerebral cortex. I. Area entorhinalis. *J. Psychol. Neurol.* **45**, 381–438 (1933).
17. R. Lorente de Nó, Studies on the structure of the cerebral cortex. II. Continuation of the study of the ammonic system. *J. Psychol. Neurol.* **46**, 113–177 (1934).
18. F. T. Lewis, The significance of the term hippocampus. *J. Comp. Neurol.* **35**, 213–230 (1923).
19. L. W. Swanson, *Neuroanatomical Terminology: A Lexicon of Classical Origins and Historical Foundations* (Oxford University Press, New York, 2015).
20. L. J. Stensaas, The development of hippocampal and dorsolateral pallial regions of the cerebral hemisphere in fetal rabbits. I. Fifteen millimeter stage, spongioblast morphology. *J. Comp. Neurol.* **129**, 59–70 (1967).

21. L. J. Stensaas, The development of hippocampal and dorsolateral pallial regions of the cerebral hemisphere in fetal rabbits. II. Twenty millimeter stage, neuroblast morphology. *J. Comp. Neurol.* **129**, 71–84 (1967).
22. L. J. Stensaas, The development of hippocampal and dorsolateral pallial regions of the cerebral hemisphere in fetal rabbits. 3. Twenty-nine millimeter stage, marginal lamina. *J. Comp. Neurol.* **130**, 149–162 (1967).
23. L. J. Stensaas, The development of hippocampal and dorsolateral pallial regions of the cerebral hemisphere in fetal rabbits. IV. Forty-one millimeter stage, intermediate lamina. *J. Comp. Neurol.* **131**, 409–422 (1967).
24. L. J. Stensaas, The development of hippocampal and dorsolateral pallial region of the cerebral hemisphere in fetal rabbits. V. Sixty millimeter stage, glial cell morphology. *J. Comp. Neurol.* **131**, 423–436 (1967).
25. L. J. Stensaas, The development of hippocampal and dorsolateral pallial regions of the cerebral hemisphere in fetal rabbits. *J. Comp. Neurol.* **132**, 93–108 (1968).
26. M. Hines, Studies in the growth and differentiation of the telencephalon in man. The fissura hippocampi. *J. Comp. Neurol.* **34**, 73–171 (1922).
27. G. E. Smith, The relation of the fornix to the margin of the cerebral cortex. *J. Anat. Physiol.* **32**, 23–58 (1897).
28. L. W. Swanson, C. Köhler, A. Björklund, "The limbic region. I: The septohippocampal system" in *Handbook of Chemical Neuroanatomy*, Integrated Systems of the CNS, Part I, T. Hökfelt, A. Björklund, L. W. Swanson, Eds. (Elsevier, Amsterdam, 1987), vol. 5, pp. 125–277.
29. T. W. Blackstad, Commissural connections of the hippocampal region in the rat, with special reference to their mode of termination. *J. Comp. Neurol.* **105**, 417–537 (1956).
30. P. Andersen, T. V. P. Bliss, K. K. Skrede, Lamellar organization of hippocampal pathways. *Exp. Brain Res.* **13**, 222–238 (1971).
31. T. V. P. Bliss, G. L. Collingridge, R. G. M. Morris, K. G. Reymann, Long-term potentiation in the hippocampus: Discovery, mechanisms and function. *Neuroforum* **24**, A103–A120 (2018).
32. N. Hopwood, *Embryos in Wax: Models from the Ziegler Studio* (Whipple Museum of the History of Science, Cambridge University, Cambridge, United Kingdom, 2002).
33. L. W. Swanson, *Brain Maps: Structure of the Rat Brain. A Laboratory Guide with Printed and Electronic Templates for Data, Models and Schematics* (Elsevier, Amsterdam, ed. 2, 1998).
34. H.-W. Dong, *Allen Reference Atlas: A Digital Color Brain Atlas of the C57Black/6J Male Mouse* (Wiley, Hoboken, 2007).
35. Allen Institute for Brain Science, Allen mouse common coordinate framework v. 3, (2017). https://scalablebrainatlas.incf.org/mouse/ABA_v3. Accessed 10 December 2019.
36. J. P. Snyder, *Flattening the Earth: Two Thousand Years of Map Projections* (University of Chicago Press, Chicago, 1993).
37. J. D. Hahn, L. W. Swanson, Connections of the lateral hypothalamic area juxtadorsomedial region in the male rat. *J. Comp. Neurol.* **520**, 1831–1890 (2012).
38. G. Alvarez-Bolado, L. W. Swanson, *Developmental Brain Maps: Structure of the Embryonic Rat Brain* (Elsevier, Amsterdam, 1996).
39. L. W. Swanson, *Brain Maps: Structure of the Rat Brain. A Laboratory Guide with Printed and Electronic Templates for Data, Models and Schematics* (Elsevier, Amsterdam, ed. 3, 2004).
40. Allen Institute for Brain Science, Allen Mouse Brain Connectivity Atlas. (2019). http://connectivity.brain-map.org/. Accessed 10 December 2019.
41. A. San Antonio, K. Liban, T. Ikrar, E. Tsyganovskiy, X. Xu, Distinct physiological and developmental properties of hippocampal CA2 subfield revealed by using anti-Purkinje cell protein 4 (PCP4) immunostaining. *J. Comp. Neurol.* **522**, 1333–1354 (2014).
42. Allen Institute for Brain Science, Allen Mouse Brain Atlas, ISH data for Pcp4. (2017). https://mouse.brain-map.org/experiment/siv?id=772&imageId=101303491&initImage=ish&coordSystem=pixel&x=1560&y=1446.5&z=1. Accessed 10 December 2019.
43. D. M. Simmons, L. W. Swanson, Comparing histological data from different brains: Sources of error and strategies for minimizing them. *Brain Res. Brain Res. Rev.* **60**, 349–367 (2009).
44. D. Fürth *et al.*, An interactive framework for whole-brain maps at cellular resolution. *Nat. Neurosci.* **21**, 139–149 (2018). Erratum in: *Nat. Neurosci.* **21**, 895 (2018).
45. L. W. Swanson, W. M. Cowan, An autoradiographic study of the organization of the efferent connections of the hippocampal formation in the rat. *J. Comp. Neurol.* **172**, 49–84 (1977).
46. L. W. Swanson, Mapping the human brain: Past, present, and future. *Trends Neurosci.* **18**, 471–474 (1995).
47. H. M. Duvernoy, *The Human Hippocampus: An Atlas of Applied Anatomy* (Bergmann, Munich, 1988).
48. L. W. Swanson, Cerebral hemisphere regulation of motivated behavior. *Brain Res.* **886**, 113–164 (2000).